J. Condensed Matter Nucl. Sci. 29 (2019) 472–492

Research Article

On Highly Relativistic Deep Electrons

Jean-Luc Paillet*
University of Aix-Marseille, 13007 Marseille, France

Andrew Meulenberg
Science for Humanity Trust Inc., USA

Abstract

We address a number of questions relating to the progress of our study on the relativistic-electron deep orbits (EDOs): (1) How to combine different EM potentials having two possible versions (attractive and repulsive), while rejecting unrealistic energies? (2) What about the angular momentum of the deep electrons? How is the Heisenberg Uncertainty Relation satisfied in these EDOs? (3) From where is extracted the high kinetic energy (of order 100 MeV) of the deep-orbit electrons? (4) What is the behavior of the effective potential V_{eff} as a function of distance to the nucleus? (5) What is the order of magnitude of the radiative corrections for the EDO's? (6) What is the relation between EDO solutions of the Dirac equation and the high energy resonances (with high binding energies) corresponding to a semi-classical local minimum of energy?
 ISSN 2227-3123

Keywords: Confinement, Deep electron levels, Heisenberg uncertainty relation, Highly relativistic bound electrons, LENR

1. Introduction

The observed generation of heat, in excess of that possible from chemical reactions, from deuterium-loaded palladium substrates at room temperature [1] led to a field of endeavor called "cold fusion". It was proposed that, as in the well-known hot ($\sim 10^7$°C) fusion processes of the sun, the embedded deuterium atoms were somehow able to come together close enough to fuse and liberate significant nuclear energy. This incredible news was initially welcomed because of the need for cheaper energy sources, the known fusion reactions, and the many decades of research supporting them. However, the extensive base of well-known and accepted nuclear physics soon became a reason that cold fusion was rejected by those knowledgeable in the field. The results of cold fusion did not agree at all with what was known from hot-fusion research. Either the cold fusion research was faulty or something new was happening. Assuming the data was correct, what was new?

Was the solid state or crystalline environment of the palladium substrate somehow able to help two deuterons overcome their Coulomb repulsion? If so, how? Many models for this mechanism were proposed, and, correctly

*Corresponding author. E-mail: jean-luc.paillet@club-internet.fr.

 ISSN 2227-3123

or incorrectly, subsequently rejected. Many of these relied on placing an electron between the deuterons for a much greater period than that of the bound atomic electrons. It was known that this was possible with a heavy electron (e.g., the muon, with $>200\times$ the electron mass); but, the known fusion of deuterium in the presence of muons resulted in the same products predicted by hot fusion, but not in cold fusion. Thus, this effect, alone, could not be the appropriate mechanism for cold fusion. Was there a mechanism that produced electron placement in such a manner as to alter the fusion process itself? Fortunately, the energy levels of the ^{4}He nucleus were well-known and could provide an answer that both depended on an electron spending more time between the deuterons and altered the products of the resulting d–d fusion reaction [2]. This answer did not explain how an electron could spend more time between deuterons; but, it is consistent with prior [3–5], and more recent [6–8], models that did so.

Classical physics allows an electron to orbit close to the nucleus for short periods, during which time the nuclear Coulomb barrier is strongly shielded. This was an approach explored for a time until it was noticed that quantum mechanics (QM), in the form of the Relativistic Klein–Gordon and Dirac equations, had predicted the existence of electron deep-electron orbits (EDOs) many decades ago. These models did not depend on spin for this prediction. The introduction of relativity into the QM equations made the difference between *only* the atomic orbitals and those *plus* the deep orbits. Unfortunately, since no deep orbits had ever been seen and the concept of the neutron as a proton plus tightly bound electron had been rejected, interest in this solution of the relativistic equations was greatly reduced. It periodically reappeared (almost every 10 years); however, because the deep-orbit solution had a singular point (at $r = 0$) when a strict Coulomb potential and point charges were considered, this portion of these important equations were regularly rejected on a mathematical basis alone.

In trying to understand a physical basis for the deep orbits, relativistic effects were examined in greater detail [9,10] and the several arguments against the EDOs were successfully refuted [11,12]. However, the greatest argument for the reality of these deep orbits is in the predictions of physical effects based on such orbits [13–20]. Once it was established that the EDOs could explain most or all of the observed cold fusion effects, it became important to look at other relativistic effects [21,22] to improve the model. Inclusion of actual nuclear details have been made as successive approximations and not all "branch" points have been explored yet.

This paper is a continuation, with a brief overview, of that study. It starts with the assumption that the Heisenberg Uncertainty Relation (HUR) applies to the nuclear range as well. From this it is possible to calculate a limit for the relativistic coefficient, γ, and, then, to look at the deep-orbit-electron's relativistic interactions with its orbit and the nuclear components (e.g., spin and charge). The greatly enhanced forces and potentials from relativity and proximity create very large energies (100 s of MeV) relative to the static calculations and yet the binding energy of the deep-orbit electron is still relatively small ($|\mathrm{BE}| < 0.511$ MeV) because it is a difference between kinetic and potential energies. Since the observables are small differences between large numbers, many assumptions and relations, made in historical work for different ranges, may no longer be valid. Thus, continued refinement, testing, and examination of assumptions and premises are required for this transition to the highly relativistic nuclear regime. An exploration of QED in this context brings another tool into the effort.

2. Relativistic Confinement Energies and the Relativistic Coefficient γ

In previous studies on magnetic interactions [22,23], we showed magnetic potentials to have very high energy near the nucleus; as a consequence, we could expect the HUR to be respected in this zone. Next, we adopted a *new strategy*: to directly address the HUR as a starting point, while considering an electron confined in a sphere of radius r.

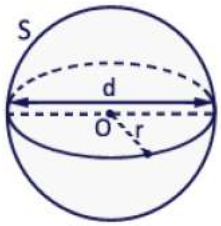

The HUR can be expressed by the inequality $\Delta p\,\Delta x \geq \hbar/2$, where p is the norm of the momentum of the considered particle and x is its radial location. The delta indicates the uncertainty in these parameters. As in most QM textbooks (see e.g. [24,25]) we can put $p \sim \hbar/r$, where the "2" has been removed, to take a reasonable average value for p based on this relation. Then, we consider the relativistic expression of momentum, $p = \gamma mv$, where m is the rest mass of the electron, v its velocity, and γ the relativistic coefficient defined by $\gamma = (1\text{-}\ v^2/c^2)^{-1/2}$. We can deduce $\gamma\ v = \hbar/mr$.

Now, by using the expression of γ, one has $(\gamma\ v)^2 = (cv)^2/(c^2 - v^2) = (\hbar/mr)^2$. From $(cv)^2/(c^2 - v^2) = (\hbar/mr)^2$ and, by simple algebraic transformations[a], we obtain $\gamma^2 \sim 1 + \hbar^2/(mrc)^2$. Recognizing the reduced Compton wavelength of the electron as a constant, $\underline{\lambda}_c = \hbar/mc$, we have relation (1), expressing γ as a function of the confinement radius r:

$$\gamma^2 \sim 1 + (\underline{\lambda}_c/r)^2, \quad \text{i.e.} \quad \gamma \sim [1 + (\underline{\lambda}_c/r)^2]^{(1/2)}. \tag{1}$$

Moreover, as $\underline{\lambda}_c \sim 386$ F for an electron, and for the EDOs, r is of order a few F, one has $r \ll \underline{\lambda}_c$, and thus $(\underline{\lambda}_c/r)^2 \gg 1$. In this case, the previous relation expression can be reduced to a very simple one:

$$\gamma \sim \underline{\lambda}_c/r. \tag{2}$$

Note that for highly relativistic velocities $v \to c$ and $\gamma^2 \sim \hbar^2/(mcr)^2$, and we have relation (2) as well. The kinetic energy, KE $= (\gamma\text{-}1)\,mc^2$, becomes $\sim ((\underline{\lambda}_c/r) - 1)\,mc^2$ and, expressed as a function of the de Broglie wavelength λ_{dB} assuming the quantum condition for the lowest closed orbit of $\lambda_{dB} = 2\pi r = 2\pi\hbar/p = h/p$, KE $\approx (\lambda_c\ /\lambda_{dB}\ \text{-}1)\,mc^2$ with $\gamma \approx \lambda_c\ /\lambda_{dB}$, where λ_c is the Compton wavelength under non-reduced form.

2.1. Examples of confinement energies at some ends of the energy scale

(1) For the case of an atomic electron, we consider r equal to the Bohr radius $r_B = \hbar/\alpha cm$, where α is the coupling constant of electro-magnetism. The kinetic energy corresponding to the confinement of an electron in a radial region corresponding to r_B is equal to $E \approx p^2/2m$, a non-relativistic expression, because we know the electron is not very relativistic (see its γ in Section 2.2). While putting $p = \hbar/r_B$, we obtain $E \approx (\hbar/r_B)^2/2m = mc^2\alpha^2/2$, which is the expression of the classical Rydberg energy, of numerical value ~13.6 eV, a well-known result associated with the ground state of the hydrogen atom and the HUR.
(2) Consider now the case where $r = 2$ F, where an electron is very close to the nucleus, as in the EDO.

We can expect the electron to have relativistic speed, requiring the relativistic expression of the energy, i.e. $E = (p^2c^2 + m^2c^4)^{1/2}$. A numerical computation shows that $pc \gg mc^2$, and so, for this near-nuclear orbit, $E \sim pc \sim 98.6$ MeV.

[a] With $s = \hbar/mr$, $(cv)^2 = (cs)^2\text{-}(vs)^2$, we deduce $v^2(c^2 + s^2) = (cs)^2$, $(v/c)^2 = s^2/(c^2 + s^2)$, $\gamma^2 = 1/(1 - (v/c)^2) = 1/[1\text{-}s^2/(c^2 + s^2)] = 1 + s^2/c^2$.

2.2. Examples of relativistic coefficients, for the confinement radii indicated in Section 2.1

(1) We consider again $r = r_{\mathrm{B}}$, as in Section 2.1 (1). Then we compute γ in two different ways.

(a) First, we know the kinetic energy is the Rydberg energy $E_{\mathrm{Ryd}} = mc^2\alpha^2/2$. But the kinetic energy KE is also given by the expression KE = (γ-1) mc^2. From KE = E_{Ryd}, we can deduce $\gamma = 1+\alpha^2/2$. From this, we have $\beta^2 = (v/c)^2 = 1\text{-}1/\gamma^2 = (1\text{-}1/(1+\alpha^2/2)^2) \sim ((1+\alpha^2/2)^2\text{-}1) \sim \alpha^2$, so $v \sim \alpha c \sim$**c**/137, a well-know result calculated by Arnold Sommerfeld.

(b) Now, we compute γ by means of the results deduced from HUR. As one has $r = r_{\mathrm{B}}$, the condition $r \ll \underline{\lambda}_{\mathrm{c}}$ is not satisfied and we use the full expression for γ (1): $\gamma \sim (1 + (\underline{\lambda}_{\mathrm{c}}/r_{\mathrm{B}})^2)^{(1/2)}$. With $\underline{\lambda}_{\mathrm{c}} = \hbar/mc$ and $r_{\mathrm{B}} = \hbar/\alpha cm$, we obtain $\gamma \sim (1+\alpha^2)^{(1/2)} \sim 1+\alpha^2/2$, while neglecting the terms of order α^{n} for $n \geq 4$. So we still have a very good approximation of the result of Sommerfeld.

(2) Consider the case $r = 2$ F. As $r \ll \underline{\lambda}_{\mathrm{c}}$, we can use expression (2) to compute $\gamma \sim \underline{\lambda}_{\mathrm{c}}/r = 386/2 = 193$, and $\beta = 0.99998\ldots$ The electron is ultra-relativistic. The question is therefore the following: can a Coulomb potential confine such an ultra-relativistic electron? We show how to solve this question positively in Section 3.

3. The Relativistic Effective Potential Energy V_{eff} is Strong Enough to Confine Electrons in Deep Orbits

Because of the high level of the relativistic coefficient γ, it is interesting to consider the effects of the relativistic correction to the static Coulomb potential, as indicated in [26,27], under the resulting form of an effective dynamical potential noted V_{eff}, and already considered in [28,10]. The general form Eq. (3) of V_{eff}, comes from the development of relativistic quantum equations (Dirac, Klein–Gordon) with the expression of the relativistic energy of a particle in a central field for a Coulomb potential energy V:

$$V_{\mathrm{eff}} = V(E/mc^2) - V^2/2mc^2. \tag{3}$$

This transformation is little known since, in the atomic cases and for light elements, we have $E \sim mc^2$ and $V \ll mc^2$ that leads to $V_{\mathrm{eff}} \sim V$. On the other hand, while considering the relativistic expression of the E of an electron in the potential V, i.e. $E = V+(\mathbf{p}^2c^2 + m^2c^4)^{1/2}$, we can deduce the following form Eq. (4), including the coefficient γ:

$$V_{\mathrm{eff}} = \gamma V + V^2/2mc^2. \tag{4}$$

Now, we put the full expression of γ (1), $\gamma \sim [1 + (\underline{\lambda}_{\mathrm{c}}/r)^2]^{(1/2)}$, into Eq. (4), to obtain V_{eff} as a function of r:

$$\begin{aligned} V_{\mathrm{eff}} &= -(\alpha c\hbar/r)([1 + (\underline{\lambda}_{\mathrm{c}})^2/r^2]^{(1/2)} - \alpha\hbar/2mcr) \\ &= -(\alpha c\hbar/r)([1 + (\underline{\lambda}_{\mathrm{c}})^2/r^2]^{(1/2)} - \alpha\underline{\lambda}_{\mathrm{c}}/2r). \end{aligned} \tag{5}$$

For r of order a few F and by reduction of γ, this expression can be simplified into:

$$V_{\mathrm{eff}} \sim (\alpha c\hbar\underline{\lambda}_{\mathrm{c}}/r^2)(1 - \alpha/2). \tag{6}$$

One can also write the following approximate (equivalent) forms, while neglecting the term $\alpha/2$ in the second parenthesis of Eq. (6):

$$V_{\mathrm{eff}} \sim \gamma V \sim (\underline{\lambda}_{\mathrm{c}}/r)V \sim \underline{\lambda}_{\mathrm{c}}e^2/r^2 \sim \alpha c\hbar\underline{\lambda}_{\mathrm{c}}/r^2 \sim -\alpha\hbar^2/mr^2. \tag{7}$$

When looking at formula (4), we can see the first term of the sum, equal to γV, which expresses a strengthening of the attractive potential V, since γ is always ≥ 1. But the second term of the sum in Eq. (4), $V^2/2mc^2$, has a positive sign, that means a repulsive action. The question is therefore whether V_{eff} is always a reinforcement of V.

- For $r \ll \lambda\!\!\!^{-}_{c}$, expression (6) allows us to answer yes.
- If we release this condition, we have to use expression (5), and this one does not allow to answer the question easily in a purely algebraic way. Previously [28], we could show V_{eff} is always a reinforcement of V, but only for quasi-circular orbits.

Now, by using a numerical method, we can show without any hypothesis on the shape of the orbit, the following result: $V_{\text{eff}} < V < 0$ when $r < 52.91741577$ pm, to compare with the Bohr radius $r_{\text{B}} \sim 52.9177210$ pm. Such precision may seem ridiculous, as the computation of γ from the HUR is based on an approximate principle and the s-orbit is nearly linear. Nevertheless, we can give the following results for V_{eff}.

With only the condition $r <\sim r_{\text{B}}$, i.e. for any energy level under the ground state and independent of any of the HUR analysis above, we have:

(1) V_{eff} is always attractive,
(2) $|V_{\text{eff}}| > |V|$, i.e. V_{eff} is always a strengthening over the static Coulomb potential,
(3) Moreover, expressions (6) and (7) show that: when r decreases sufficiently and $\to 0$, V_{eff} has a behavior in K/r^2, with $K \sim 8.9 \times 10^{-41}$ SI units, i.e. Jm^2.

Finally, and most importantly for the EDO's, if computing V_{eff} near the nucleus, e.g. for r ~2 F, we have $\gamma \sim 193$, as indicated in Section 2.2, and we obtain $V_{\text{eff}} \sim -139$ MeV, whereas the kinetic energy KE $= (\gamma - 1)\, mc^2 \sim 192 \times 511$ keV ~ 98 MeV. With such a high value, V_{eff} can easily confine an electron in this region.

In [10], we showed that Special Relativity is the source of the EDO's. Now, we show that the HUR, which seemed an impediment for the EDO's, provides its proper resolution thanks to relativity.

4. Looking for a Resonance Near the Nucleus

The deep orbit electrons have the following features:

- They are highly relativistic.
- They are subjected to several electro-magnetic interactions of high intensity, some of which are not involved in the Dirac equation used until now for determining the EDOs for a single particle.
- Note also that, in the "nuclear zone", the deep-orbit electrons are certainly subject to fairly high radiative corrections. But the Coulomb electric field, strengthened by a relativistic effect corresponding to V_{eff}, seems sufficient by itself to retain an electron in the nuclear zone.

Under these conditions, the question of EDO stability seems a very difficult problem to solve. Nevertheless, to have a first estimate of a possible stable resonance, we can use a well-known semi-classical approximation, which consists of seeking a local minimum of energy (LME), in an approximate way similar to that used for finding the ground state, the Bohr level. One can find this in most Quantum Mechanics textbooks, e.g. [24].

In fact, we combine two approaches for doing this:

- To attempt to determine which interactions have the greatest role(s) in generating a resonance.
- To compute a total energy, while respecting the HUR.

For the latter point, we consider the relativistic expression of energy, in which the norm of momentum $|\mathbf{p}|$ is replaced by $\hbar/r$, that gives the following expression, denoted E_{H} (H for Heisenberg):

$$E_{\text{H}} = \sqrt{\frac{\hbar^2 c^2}{r^2} + m^2 c^4}. \tag{8}$$

With relation (1), $\gamma \sim [1 + (\underline{\lambda}_c/r)^2]^{(1/2)} = [1 + \hbar^2/(mcr)^2]^{(1/2)}$, one easily verifies that the kinetic energy KE = (γ-1) mc^2 is also equal to $E_H - mc^2$. Indeed

$$\text{KE} = mc^2[1 + \hbar^2/(mcr)^2]^{(1/2)} - mc^2 = [m^2c^4 + \hbar^2c^2/r^2]^{(1/2)} - mc^2 = E_H - mc^2. \quad (9)$$

In principle, we add to E_H, a term V representing a potential energy, where V is a function of the radius. Thus we obtain the total energy E, represented by the following relation: $E = E_H + V$. Then, we look for an LME for various combinations of potentials included in the term V and we determine the radius of this local minimum. Of course, V systematically includes the dynamical effective potential V_{eff}, given its essential role for the existence of EDOs indicated in Section 3. But, before developing the question of the combination of potentials included in V, it is interesting to look at the properties of the "minimal combination", by putting $V = V_{\text{eff}}$ and thus $E = E_H + V_{\text{eff}}$.

4.1. Study of the case, where the only potential taken into account is the effective potential V_{eff}

In this section, we have PE = V_{eff} and $l = 0$.

First, we plot below (Fig. 1) three curves: $|V_{Cb}|$, $|V_{\text{eff}}|$ and KE = $E_H - mc^{2\cdot}$, in loglogplot. The static Coulomb potential is denoted by V_{Cb}, to avoid confusion with the combination of potentials V. To make it easier to read the calculation results, we put $r = \rho \times 10^{-12}$ and we compute with ρ.

In this figure, we can observe the following:

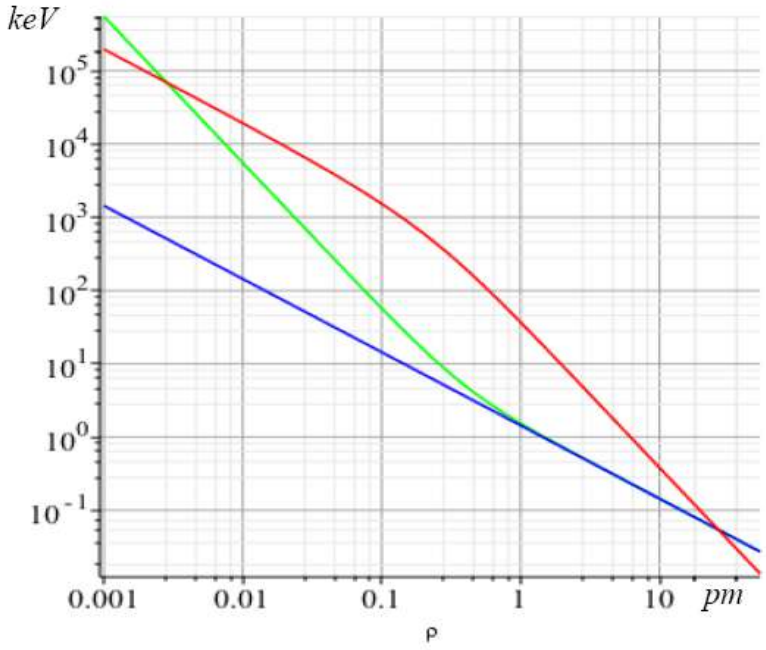

Figure 1. Loglogplot of energies (in keV) for radius denoted by ρ in pm, where 1 F< ρ < 53 pm. (*Blue*) norm of Coulomb potential $|V_{Cb}|$, (*Green*) norm of the effective potential $|V_{\text{eff}}|$, and (*Red*) kinetic energy KE.

(1) $V_{\rm eff}$ is always a strengthening of $V_{\rm Cb}$, as indicated in Section 3. In the figure, because of the extent of the scale in loglogplot, $V_{\rm eff}$ is indistinguishable from $V_{\rm Cb}$ at high ρ values and only separates when ρ decreases and reaches 1 pm.
(2) $|V_{\rm eff}|$ and KE intersect at two points, near the ends of the radius scale in Fig. 1. The numerical solution of the equation $|V_{\rm eff}| = {\rm KE}$ gives these points: ∼26.45 pm and ∼2.828 F, approximated in the figure. For a non-relativistic orbit, the virial theorem states KE = |PE|/2. Thus, the Bohr radius at this stable point is ∼53 pm. For relativistic orbits, KE = $|{\rm PE}|\gamma/(\gamma+1)$ and KE → |PE| as $v \to c$, and 2.83 F is near the classical electron radius (∼2.82 F). This is not a simple coincidence.[b]

Most important is the presence of both crossing points of the curves of KE and $|V_{\rm eff}|$, 2.82 F and 26.5 pm, indicating the possibility of resonance in two regions, where $|V_{\rm eff}|$ becomes stronger than KE:

- either for $\rho > 26.5$ pm: in this area, there are the well-know atomic energy levels, whose lowest is the ground level (Bohr) at ∼53 pm, where $V_{\rm eff} \sim V_{\rm Cb} = -2$ KE ∼ −26 eV,
- or for $\rho < 2.8$ F, where we might expect resonance of type "EDO".

Of course, when taking into account further EM interactions near the nucleus, this limit $\rho < 2.8$ F could move slightly. We say "slightly", because the energies of the interactions, considered further, are relatively small compared to $V_{\rm eff}$ and KE, where we set aside huge, physically "unreasonable," interactions for the orbits of present interest.

Another important, but difficult, question concerns the possibility of transition between the "atomic" zone and the "EDO" zone. We will give some reflections on this further question. Nevertheless, while considering the $E = E_{\rm H} + V_{\rm eff}$ and the derivative $\mathrm{d}E/\mathrm{d}\rho$ to find possible local extrema of E by solving $\mathrm{d}E/\mathrm{d}\rho = 0$, we find as follows.

(1) An obvious local minimum at $\rho = r_{\rm B}$ ∼52.9 pm, for the atomic ground state.
(2) A local maximum at ρ ∼5.6 F, where KE + $V_{\rm eff}$ ∼17 MeV, that represents a high "pseudo-barrier" for a transition from atomic zone to EDO zone. We can call it the "Heisenberg barrier", since it is due to the very-high kinetic energy required by HUR. In fact, at this radius, we have: KE ∼34.6 MeV, while $V_{\rm eff} \sim -17.6$ MeV. Thus, the barrier is 34.6–17.6 MeV ∼17 MeV. On the other hand, below the EDO zone, E becomes negative and continuously decreases towards $-\infty$. Under these conditions, the existence of further repulsive interactions is necessary to generate a resonance. We represent, in Fig. 2, the plotted curve of KE + $V_{\rm eff}$ with a radius scale adequate to observe the maximum and the behavior for ρ very small.
Remark: KE+$V_{\rm eff}$ has the same behavior as E and extrema have the same location, since $E = {\rm KE} + V_{\rm eff} + mc^2$.

4.2. What combination of potentials to consider, for finding a deep LME?

From our previous works on magnetic interactions [22,23], including the study of the Barut–Vigier model and related works, we are led to some conclusions about combinations of potentials capable of producing a LME near the nucleus.

(1) In particular, it seems that we have to rule out the possibility of a *spin–orbit interaction* for an electron in the EDO zone: indeed, the energy $E_{\rm SO}$ associated with the spin–orbit interaction is given by the following expression

$$E_{\rm SO} = \frac{\mu_0 e^2}{8\pi m^2}\frac{1}{r^3} L{\cdot}S = \xi(r) L{\cdot}S, \tag{10}$$

[b]Let us calculate for which value of radius r we have the maximum possible value of |BE|, i.e. BE $= -mc^2$, *while supposing we are in a resonance case*. With BE = KE + PE, and the approximate expression (7) for $V_{\rm eff}$, we have $-mc^2 \sim (\gamma-1)mc^2 + \gamma V_{\rm Cb} \to V_{\rm Cb} \sim -mc^2$, i.e. $\alpha ch/r \sim mc^2$, $r \sim \alpha ch/mc^2$. This is the expression for the electron classical radius $r_{\rm e}$. Somehow $r_{\rm e}$ is a limiting radius for a resonance under the hypothesis PE $= V_{\rm eff}$.

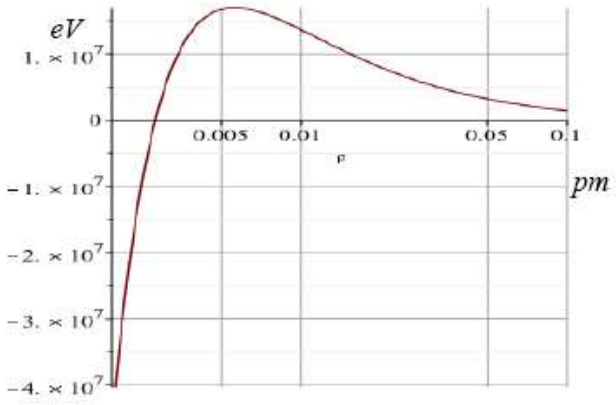

Figure 2. Semilogplot of KE+V_{eff} (in eV) with ρ in pm, for 2 F < ρ <0.1 pm.

where, for any value of the quantum angular momentum $l \neq 0$,

- the attractive case corresponds with $L{\cdot}S = -(\hbar^2/2)\,(l{+}1)$,
- while the repulsive one, with $L{\cdot}S = +(\hbar^2/2)\,l$.

But, previous computations of the energy E_{SO} associated with the spin–orbit interaction in attractive mode, while supposing l =1 and applying the usual quantization rules, give $E_{\text{SO}} \sim -13$ GeV for an electron at a distance $r \sim$2 F, i.e. in the expected region of the EDOs. Such a huge value does not seem physically reasonable and this term would prevent a bound state. If considering the repulsive case, with l =1, the formulas above show we obtain one half of the previous value, i.e. 6.5 GeV, which is still physically unreasonable. Under these conditions, one has to consider the angular momentum to be $l = 0$.

(2) Moreover, if $l = 0$, there is no *centrifugal (repulsive) potential*, since this is proportional to $l(l{+}1)$ in the quantum formulations (e.g. the relativistic Schrödinger equation, [29]) and we can think the orbit is essentially linear through, or (if a hard core exists) at least toward, the nucleus.

(3) As a consequence, to balance the attractive potential energy V_{eff} and to expect a resonance near the nucleus, we have to consider the *repulsive version* of the *magnetic spin–spin interaction* (i.e. the triplet state), denoted by V_{RSS}. Here, we recall that the spin–spin interaction can be expressed by the following general formula (see e.g. [30,31]):

$$H_{\text{SS}} = -\frac{\mu_0}{4\pi}\left[\frac{1}{r^3}\left(3\left(M_{\text{p}}\cdot\hat{r}\right)\left(M_{\text{e}}\cdot\hat{r}\right) - M_{\text{p}}\cdot M_{\text{e}}\right) + \frac{8\pi}{3}M_{\text{p}}\cdot M_{\text{e}}\delta\left(r\right)\right], \tag{11}$$

where M_{p} and M_{e} are the magnetic moments of the proton and the electron, respectively and $\hat{r}$ denotes a radial unit vector. The magnetic moments are related to the respective electron and nuclear (i.e. proton, here) spins S_{e} and S_{p} by the following formulas:

$$M_{\text{e}} = (e/2m_{\text{e}})S_{\text{e}} \quad \text{and} \quad M_{\text{p}} = (2.79|e|/m_{\text{p}})S_{\text{p}}. \tag{12}$$

By introducing the total spin $S = S_{\text{e}} + S_{\text{p}}$ and discounting anyrelativistic effects for the moment, one can write the following relation:

$$S_{\text{e}}{\cdot}S_{\text{p}} = (1/2)(S^2 - (S_{\text{e}})^2 - (S_{\text{p}})^2) = (\hbar^2/2)[s(s+1) - 3/2]. \tag{13}$$

The only possible values of s are $s = 0$ ("singlet" state) and $s = 1$ ("triplet" state), which gives two cases:

- $s = 0 \Rightarrow S_e \cdot S_p = -(3/4)\hbar^2$, i.e. "attractive case",
- $s = 1 \Rightarrow S_e \cdot S_p = +(1/4)\hbar^2$, i.e. "repulsive case".

While extrapolating the known values of spin–spin interaction energy computed at the Bohr radius, to a general expression of the spin–spin interaction energy for any radius r. We found [23], for the repulsive spin–spin (RSS) version noted V_{RSS}, $V_{\mathrm{RSS}} \sim 3.4 \times 10^{-56}/r^3$ SI, i.e. J/m^3. For example, for $r \sim 5$ F, we have $V_{\mathrm{RSS}} \sim 2.7 \times 10^{-13}$ J $\sim$1.7 MeV.

Note that, for a particle in a relativistic regime, the spin tends to lean in the direction of the motion of the particle [32] and *we could think that it leads to a weakening of the effect on* V_{RSS}.

(4) We have also to take into account a further interaction, always present and repulsive. We recall this term is caused by an interaction between the magnetic moment of the electron with the charge of the proton and involves the squared norm of the magnetic vector potential of the electron,

$$\mathbf{A}\,(r) = \frac{\mu_0}{4\pi}\frac{\mathbf{m} \times \widehat{r}}{|\mathbf{r}|^2},$$

where $\mathbf{m}$ is the magnetic moment of the electron. The complete energy term associated with $\mathbf{A}^2$ has the form $e^2\mathbf{A}^2/2m$ and is considered [33,34] to be expressing a *diamagnetic* energy with a behavior in $1/r^4$. The energy of this diamagnetic interaction, noted V_{dia} and although very weak compared to $V_{\mathrm{RSS},}$ has to be included in the combination of potentials. We found [22,23]

$$V_{\mathrm{dia}} = K_4/r^4, \quad \text{with } K_4 = \left(\frac{\mu_0}{4\pi}\right)^2 \frac{\mathbf{e^4}\hbar^{\mathbf{2}}}{4m_e^2 m_p},$$

where m_e is the electron mass, m_p the proton mass, and $K_4 \sim 1.3 \times 10^{-71}$ SI units, i.e. J m^4. *Again, relativistic effects on the spin vector orientation could reduce the values obtained for* $\mathbf{m} \times \mathbf{r}$.

In Appendix 1, we give elements of discussion about magnetic interactions for relativistic electrons.

4.3. Effects of radiative corrections

We have to take into account the effects of radiative interactions, which are strong in the nuclear area.

On one hand, some EM interactions become very strong when the radius decreases because of behavior in inverse powers of r, mostly in powers -2, -3 and -4 for V_{eff}, V_{RSS} and V_{dia}, respectively. On the other hand, *radiative corrections*, which are specific EM interactions deduced from the quantization of the EM field, have to be taken into account, as they can modify the intensity of the EM interactions considered so far.

4.3.1. *Some rudiments about radiative corrections*

The radiative corrections are determined in the framework of the Quantum Electrodynamics (QED), the first theory where QM and Special Relativity are combined in the most suitable manner, i.e. in a covariant way (see e.g. [35]). Moreover, on account of relativity, QED implements an additional quantization of a new kind, the mis-named "2nd quantization", where it is applied to the numbers of considered particles, as particles can be created or destroyed (because of the matter–energy equivalence). Moreover, it implements also the quantization of the EM field, in a way similar to a system of independent harmonic oscillators, with ladder operators of destruction/creation. QED is a fully achieved theory, as it has undergone intense development for decades, mainly in the analysis of interactions involving

free leptons and photons, occurring during scattering experiments. In principle, QED includes all relativistic effects, since any fermion quantum field is based on Dirac theory.

In brief, an electromagnetic scattering is associated with the transitions between an initial composite state to a final one, where a transition is caused by various interactions between the initial leptons and possibly photons. It is completely determined by computing the scattering matrix (or S-matrix), whose elements are the probability amplitudes for transition from an elementary initial state to a final one. The various interactions are usefully represented by Feynman diagrams, as they constitute a true algebraic coding for computing and combining all the various operators and propagators involved in the S-matrix elements. At each vertex, the sum of all the momenta is null, to express momentum conservation. Note that, generally, real particles are virtually destroyed in inputs of a transition, while various real particles can be virtually created at the outputs, and intermediate energy propagation is done by means of virtual photons.

Most important elements for the success of QED are that any transition can be decomposed into a series, thanks to a Dyson expansion of the general evolution operator (or "S operator"), and the Wick's theorem applied to the Dyson expansion that permits a finite, fully covariant, expression at any order of expansion. This makes QED a perturbation theory, i.e. it obtains successively more accurate descriptions by computing the S-matrix at an increasing order of the perturbation (of course, at the expense of a quick increase of the computation complexity). Finally, mathematical and computational complexity arises at higher orders, principally, because of loops in the Feynman diagrams: indeed, in a loop, the momentum cannot be determined by the conservation law. So, one has to consider all possible values by summing from 0 to ∞. This implies the presence of diverging integrals and led to the difficult, but efficient, methods of renormalization to overcome this obstacle.

As mentioned above, QED has been principally developed in the framework of scattering theory. It has been much less often applied to bound states, like atomic states; moreover, it seems harder to apply (less suitable?) for these states. We can cite, in the case of bound states, the approximate methods of the "Theory of the external field", particularly developed in [36] and derived from works of Furry (e.g. [37]). Summarily, in the concept of an "external field", the nucleus does not directly participate to scattering as a particle, but only the EM field generated by the nucleus is taken into account, with exchanges of (possibly virtual) photons. As famous examples of problems solved by QED in bound states, that contributed to its huge success, we can cite: the computation of the "anomalous magnetic momentum of the electron", "the Lamb shift in the hydrogen-like atoms", "the radiative transitions between bound states", as well as the analysis of "Bremsstrahlung". While these are small effects, relative to the masses involved, and therefore fit into the perturbative regime of QED that may not be valid for the nuclear interactions, their exploration may be instructive as we move toward the nucleus where the effects would be large.

4.3.2. *The Lamb shift*

For the subject of our work, i.e. the study of possible resonance near the nucleus, we are mainly concerned with the question of the Lamb shift (see e.g. [35], Section 9.6.2). Historically [38], the Lamb shift is a small energy splitting, observed between the $2S_{1/2}$(n =2, l =0, j =1/2) and the $2P_{1/2}$(n =2, l =1, j =1/2) orbitals of H atom. However, these two different levels are degenerate for the Dirac equation, i.e. have the same energy as solutions of the equation, since their energy depends only on n and j, and not on l. Nevertheless, observation gives an extra energy of order 4.4 μeV for the 2s, compared to the 2p, orbital. This is due to the fact that an S orbital enters the nuclear domain where the electric field is very high; but, because of the centrifugal potential (associated with angular momentum l =1), a P orbital does not penetrate to that region. A similar energy shift exists for the 1S orbital, between the energy computed according the Dirac equation and the observed energy level, but with a greater value $\sim$35 μeV.

Remark: the extra energy associated with the Lamb shift corresponds in fact to *a decrease of the binding energy*:

Lamb shift has a global repulsive effect on the bound electron.

Hans Bethe was the first [39] to give an approximate, non-relativistic, derivation of the Lamb shift from the concept of self-energy of the bound electron (see Section 4.3.3). The computations of Lamb shift are very complex, requiring use of the whole arsenal of QED in the difficult case of a bound state. In principle, the computations are divided into two parts:

- one part using the approximate methods of the "Theory of the external field", or "free interaction picture",
- another part with a bound representation, the so-called "Bound Interaction Picture" (BIP).

There are very few complete demonstrations in Quantum Field Theory textbooks or courses: we can cite

- a rigorous treatment in [36] including some non-relativistic approximation,
- a derivation announced as relativistic in the course of Dyson [40] but, with a non-relativistic dipole approximation, the BIP part is not covariant.

The difficulties of Lamb shift computations are due, in particular, to the fact they involve Feynman diagrams of higher order, i.e. including loops.

4.3.3. *Feynman diagrams for Lamb shift at lowest order*

Here, we show diagrams including only one loop.

There are two kinds of phenomenon involved in the Lamb shift:

- "Electron Self-Energy"(SE), corresponding with the diagram in Fig. 3. One can show (and observe) that it has a repulsive effect on the bound electron.
- "Vacuum Polarization"(VP), sometimes called also "photon self-energy", corresponding to the diagram in Fig. 4. It has an attractive effect on the bound electron. VP leads to a shell of pairs (e^-, e^+) around the bound electron, which leads to a screening effect. From the remark above, one can already deduce the effects of SE are stronger than those of VP.

Of course, such diagrams represent algebraic QED terms occurring in the Dyson expansion, after applying Wick's theorem. Moreover, the self-energy is associated with a *mass-renormalization*, whereas the vacuum polarization with a *charge renormalization*. Here, we do not write QED terms and we do not develop renormalization methods, because it is far beyond this paper.

Both phenomena of the Lamb shift are completely determined from a mathematical point of view, in the QED theory. Nevertheless it is almost impossible to find, in the literature, simple and understandable physical interpretations.

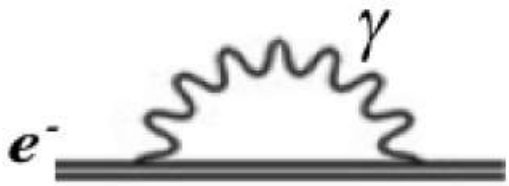

Figure 3. Electron Self-energy. e^- represents an electron, γ represents a (virtual) photon, emitted and reabsorbed by the electron. The thick line represents the fact that the electron is bound.

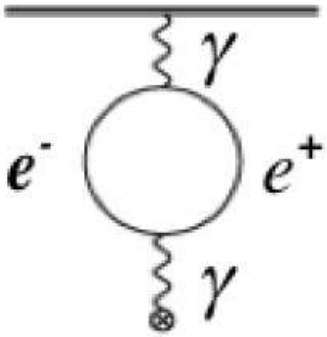

Figure 4. Vacuum polarization. e^- represents an electron, e^+ represents a positron, a photon (represented by γ) is emitted, at the bottom, by the nucleus (indicated by a cross), it produces a virtual lepton pair (e^-, e^+), this pair recombines by emitting a photon, which reaches a bound electron (not indicated).

At least for SE, we propose the following interpretation, maybe a bit simplistic, but corresponding to a well-known and clear physical concept, *the action–reaction* principle: any electrically charged particle acts on its environment by creating an EM field around itself and then, reciprocally, the so-modified environment reacts on this EM field of the particle. The acceleration of a bound particle increases this bound EM (evanescent) field that, as a standing wave, has an outgoing and a return component. The development of a magnetic field (bound to the charge) when moving is the additional energy. Likewise, any distortion of the electrostatic field (the least-energy distribution of a charge at rest) is an increase in the bound-field energy of moving charge.

For VP, a possible interpretation could be more complex, as the environment considered is the (sometimes polemical) "quantum vacuum", including energy fluctuations with creation/destruction of virtual pairs of particle–antiparticle. These energy fluctuations composed of oscillating electric fields interact with the steady-state charge fields of electrons and nuclei. The steady-state fields will polarize the oscillating fields resulting in transient charge separation and a reduction in the steady-state far-field. This effect is observed in the special case of polarization of energetic photons [41] in the creation of real electron-positron pairs where the energy and separation of the charge fields is permanent. Again, if the conditions are not "correct" for complete and stable separation, the polarized waves (virtual pairs) simply recombine as part of a reversible process.

4.4. How can we express the effect of Lamb shift on EDO's binding energy at resonance?

Despite the numerous studies of lamb shift on hydrogen-like ions with more and more precise results, this question is very difficult for several reasons:

- There is no fully analytical formulation of the two effects (SE, VP) of the Lamb shift: we indicate, below, a well-known expression of SE for the fundamental level. It includes a multiplicative factor $F(Za)$, which is given only by means of tables (see e.g. [42,43]): $\Delta E_{\mathrm{SE}} = (\alpha/\pi)(Z\alpha)^4 \mathrm{F}(Z\alpha)mc^2$. For VP, there are mainly asymptotic formulations (short/long ranges) based on Uehling potential [44].
- The computations suppose energies, which are not, or only slightly, relativistic (case of heavy elements), whereas EDO's are highly relativistic.
- From tables [45], the ratio of relative effects $|\mathrm{VP/SE}| < 1$, but it is variable: it seems to increase with Z, certainly because the s-orbital electrons are spending more time closer to the nucleus. For example: for H, $|\mathrm{VP/SE}| \sim 0.025$, whereas for ion U^{+91} one has $|\mathrm{VP/SE}| \sim 0.27$.

While continuing our study with comparisons and extrapolations from tables, and awaiting more suitable results in the future, we present here our approximate results of an LME computation.

According to our discussion on magnetic interactions (Appendix 1), we recall that we take into account two possibilities concerning the effect of magnetic interactions for highly relativistic electrons:

(a) Either, the magnetic moment of the electron is unchanged or little changed by Special Relativity and, in this case, the LME computation is performed by combining potentials indicated in Section 4.2, where the Lamb shift effects are simulated by weakening the near–nuclear interactions.
(b) Or, the spin magnetic moment is considerably weakened for highly relativistic electrons and, in this case, we compute a LME by considering the attractive potential energy $V_{\rm eff}$ and a repulsive quasi-potential energy deduced from the Lamb shift.

4.4.1. *Computations and results in the first case (a) with magnetic interactions*

Without reporting tedious details of our calculations, we can indicate the following:

- For the repulsive effect of SE, we simulate a linear weakening $V_{\rm Cbw}(r)$ of the static (attractive) Coulomb potential $V_{\rm Cb}(r)$, by a coefficient K when approaching the nucleus, i.e. at a radius $r_1 > r_0$, where r_0 is the charge radius of the nucleus ∼0.84 F. Next we deduce the dynamical effective potential $V_{\rm effw}$ from $V_{\rm Cbw}$.
- For the attractive effect of VP, we simulate a weakening of the repulsive magnetic potentials $V_{\rm RSS}$and $V_{\rm dia}$, by putting $E = E_{\rm H} + V_{\rm effw} + V_{\rm RSS}/C + V_{\rm dia}/D$, where C and D are constants >1.

Note the choice of only the repulsive version, $V_{\rm RSS}$, of the spin–spin interaction, has been made from computing experience. Moreover, while seeking a LME for resonance, we try to check an important question not yet evaluated in previous works: *is the binding energy* (BE) *of an electron caught in this resonance consistent with that predicted by relativistic equations?* To satisfy this condition, we must have at least −511 keV< BE<0. Moreover, for an EDO, one can expect a "rather high" value of |BE|.

Numerous calculations, based on the expression of the total energy E indicated above, i.e. $E = E_{\rm H} + V_{\rm w}$, where $V_{\rm w} = V_{\rm effw} + V_{\rm RSS}/C + V_{\rm dia}$/D, and with coefficients of weakening still arbitrary, confirm the possible existence of LME close to the nucleus. Moreover, we can also verify that the BE of an electron in the LME, has a "suitable" value, i.e. of the order of magnitude close to the solutions of the Dirac equation.

In Fig. 5, we display an example of the curve BE $= E - mc^2 = E_{\rm H} - mc^2 + V_{\rm w} =$ KE $+ V_{\rm w}$ to clarify the value of electron BE in the LME. For the same purpose, we restrict the scale of abscissa for the radius, denoted by ρ in fermi, while the energy values are in keV. The LME corresponds to ρ ∼1.63 F, where BE ∼ −470 keV, KE ∼120.58... MeV and PE $= V_{\rm w} \sim -121.05...$ MeV. Note the relativistic virial theorem [46] is satisfied: with precise computed values, we have KE/|PE| $= 0.996...$, $\gamma = 236.96...$ and $\gamma/(\gamma+1) = 0.9958... \sim$ KE/|PE|.

4.4.2. *Computations and results in the second case (**b**), without magnetic interactions*

We indicate in Appendix 2 some elements of principle, about the determination of a repulsive quasi-potential $V_{\rm LS}$ that we deduced from the Lamb shift for EDOs in a recent unpublished study. Here we report only results of the computation where we considered the total energy $E = E_{\rm H} + V$, with $V = V_{\rm eff} + V_{\rm LS}$ and $V_{\rm LS} \sim 6.23 \times 10^{-56}/r^3$ SI. Several computations, made while varying values of decimals, show the existence of an LME, where the binding energy BE of the electron satisfies -511 keV $<$ BE < 0 and can have value of the order of magnitude close to EDO solutions of relativistic equations.

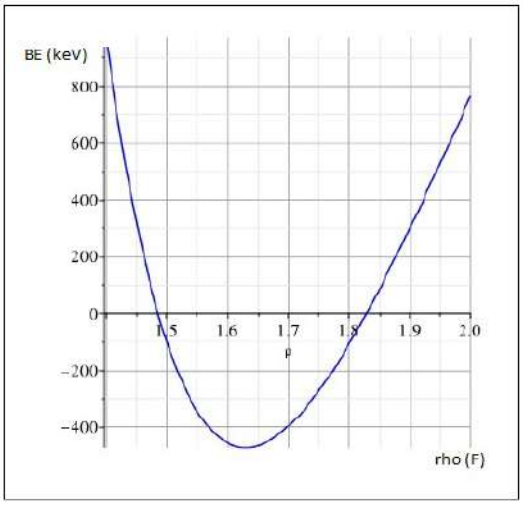

Figure 5. Plot of electron BE for 1.4 F< ρ < 2 F.

In Fig. 6, we plot an example of the curve BE, where the LME corresponds to $\rho \sim$1.41 F, BE $\sim -$ 487 keV, KE $\sim$ 140.03... MeV, PE $= V \sim$ -140.52... MeV, $\gamma =$ 275.00... We also verify that the relativistic virial theorem is satisfied.

5. Summary and Discussion of Results

(1) At this point, we can relate the results obtained for deep LME, even if only approximate, with the EDO solutions of the Dirac equation.

- In the situation considered in Section 4.4.1. while varying attenuation parameters of the EM interactions, we obtained LME locations between 1.1 F and 2 F and, on the other hand, the mean radii of EDO's obtained by the Dirac equation [21] are from 1.2 to 1.6 F, except for the value obtained when the radial quantum number $n' = 1$. Similarly, in the situation Section 4.4.2, while varying the precision of formulas, we obtain similar LME locations. Finally, in both alternatives considered from our discussion on magnetic interactions, the results have comparable orders of magnitude.
- Seeking an LME, with fixed potentials, provides only one value corresponding to an energy well, whereas the Dirac equation provides an infinity of EDOs levels. But, it is the same when one seeks the size order of electron LME in the simple Coulomb potential of a proton, as e.g. in [24]: one finds the fundamental Bohr level at 53 pm, whereas the Schrödinger equation provides an infinity of energy levels, including the fundamental level plus excited levels corresponding to additional resonances.
- In Section 4.2. (3) on *spin–spin interactions*, we noted that in a relativistic regime, the spin tends to lean in the direction of the motion of the particle [32], i.e., it is getting closer to the helicity, and we wondered if this does not lead to a weakening of the interaction energy. But, in fact, this interpretation assumes the movement of the electron becomes more perpendicular to the direction of the spin of the nucleus, as in the classical image of an orbit on the ecliptic of a planetary system. Of course, there is no reason for

the moment of the electron to have any preferred direction with respect to the orientation of the nuclear spin: one could think that spins tend to align by magnetic coupling, for reaching a lower energy state. Nevertheless, because of quantum mechanics rules on energy transfers, things are more complicated. The evolution of a system of two spins in interaction is precisely described in [47]: under the effect of the coupling, both spins process about their resultant J, with an angular velocity proportional to |J| and the coupling factor.

(2) For our calculations in the previous section, we have taken into account combinations of high-energy, $1/r^n$, potentials that are partially converted into actual kinetic energy for deep electrons. So, we have energies of order 100 – 200 MeV, while we have systematically eliminated potentials that give unrealistic energies (of order of GeV) due to angular momentum effects (spin–orbit interaction and "centrifugal potential"). Nevertheless, we can legitimately ask where do these high energies come from? The most plausible answer is that this energy is taken from the rest mass of the proton, which is of order 1 GeV. Different hypotheses exist about what constitutes the mass of a proton. Most known, from experiment in the LHC [48] and from electron–proton inelastic scattering (e.g. [49]), is that a proton is actually a "soup" of quarks, antiquarks, and gluons in a perpetual shuffling (creation/destruction of pairs) and in highly relativistic movement, but including two up-quarks (with "base" mass ∼2.4 MeV, [50]) and one down-quark (with "base" mass ∼5 MeV), named "valence" quarks. In this vision, the mass of a proton would come mainly from the relativistic energy of its constituents. In another point of view, based on the "Constituent Quark Model" [51]: in the low-energy limit of Quantum Chromodynamics (QCD), which concerns the current atomic nuclei, the constituent quarks appear like "dressed" current quarks, i.e. current quarks surrounded by a cloud of virtual quarks and gluons. This cloud underlies the large constituent-quark masses, of order 336–340 MeV. In this model, energy could still

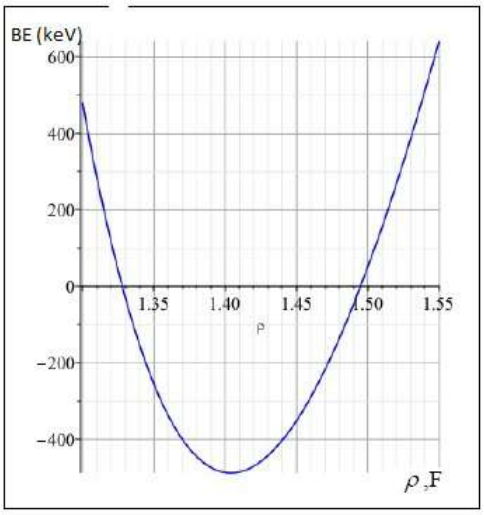

Figure 6. Plot of electron BE for 1.3 F$< \rho <$ 1.55 F.

be taken from the clouds surrounding the current quarks. Of course, the process of energy transfer from the proton-reservoir to the relativistic deep electron, with its proximate intense fields, should be the subject of a detailed study.

(3) In this paper, seeking an LME with fixed potentials is a preliminary study, carried out in a semi-classical way and with a rather coarse view of the effects of radiative corrections (essentially Lamb shift) involved near the nucleus. We are currently pursuing a study to express in a more detailed and semi-analytical manner the involvement of the Lamb shift in the computation of the resonance.

Here, we do not claim to prove rigorously that there is an LME, but we show that the existence of an LME is possible if some conditions are met (related to the combinations of potential energies). And, what is encouraging is that many calculations lead to this possibility, with a BE consistent with that predicted by relativistic equations [21]. Moreover, the resonance is confirmed by the fact that KE and PE satisfy the relativistic virial theorem.

Appendix A. Discussion about Magnetic Interactions for Relativistic Electrons

The magnetic interactions, such as spin-spin and the diamagnetic term (Section 4.2), involve the magnetic moment of the electron associated with its spin. For a relativistic electron, one knows [32] that, when the velocity increases, the direction of the spin tends to become parallel to the momentum **p**, like helicity, which can lead to a weakening of the magnetic interactions. But recently, a referee caught our attention on the fact that the magnetic moment of the electron decreases in inverse proportion of its energy. Also, and although very few documents deal with this question, we ended up actually finding papers [52,53], where the magnetic moment is given (or equivalent forms) by the relation $\mathbf{m} = e\hbar c/2E(\mathbf{p})$, where $E(\mathbf{p})$ is the total energy of an electron having momentum **p**. We note this result is deduced by reasoning of Dirac spinors in a simplified situation, i.e. for a free electron, or a electron moving in a constant magnetic field. What can be deduced for a electron bound in central potential V, a combination of several fields including a nuclear Coulomb field?

(a) On one hand, the total energy is given by $E(\mathbf{p}) = (m^2c^4 + p^2c^2)^{(1/2)} + V$. But for deep electrons, we expect a high binding energy |BE| (in absolute value) of several hundred keV [9–11,21], near the rest mass m, thus $E(\mathbf{p}) \ll mc^2$. As a consequence, we would have $\mathbf{m} \gg e\hbar/2mc$ and maybe a major strengthening of the magnetic interactions. However, while the effective **m** may be greatly increased because of relativity, the reorientation of the electron spin axis greatly decreases the $\mathbf{S} \cdot \mathbf{S}$ relation (as well as $\mathbf{L}\cdot\mathbf{S}$, for $l = 1$). It may compensate exactly and thus using $\mathbf{m} = e\hbar/2mc$, without correcting for the $\mathbf{S}\cdot\mathbf{S}$ decrease, might be a good assumption.

(b) On the other hand, we can consider the following equivalent form of the expression $\mathbf{m} = e\hbar c/2\mathrm{E}(\mathbf{p})$: $\mathbf{m} = e\hbar/2\gamma mc$, where γ is the usual relativistic coefficient. Can we consider that we have essentially to take into account the role of γ for determining the value of **m**, for a free electron *as well as a bound electron*? As a consequence, since deep electrons are highly relativistic, **m** would be very small and the magnetic interactions would be negligible compared to V_{eff}.

For the present paper, as it is very difficult to know what is the correct alternative for deep electrons, we consider both alternatives. More precisely, we are taking into account an additional effect, that of the radiative corrections, very important near the nucleus, for which we give some indispensable elements of explanation in Section 4.3.

(1) Then, while dealing with alternative (a), we keep the usual expression $\mathbf{m} = e\hbar/2mc$, and we put the total energy E equal to $E = E_{\mathrm{H}} + V$, where V will be a combination of three potential energies, V_{eff}, V_{RSS}, and V_{dia}, taking into account the effect of radiative corrections.

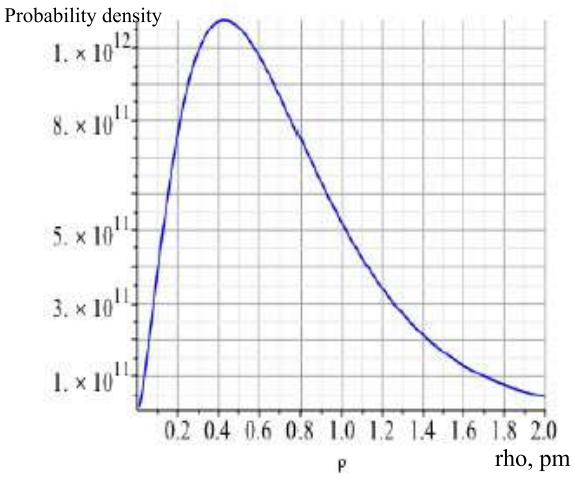

Figure 7. Plot of the normalized radial probability density for 1s orbital of uranium, for $\rho < 2$ pm. The maximum corresponds to $\rho \sim 0.43$ pm.

(2) In the case of alternative (b), we will give an overview of a possible treatment where the magnetic interactions, being considered negligible compared to the attractive interaction V_{eff}, are not taken into account. But, the potential well needed for the existence of deep electrons can still be achieved thanks to a repulsive quasi-potential deduced from the Lamb shift and combined with V_{eff}.

Appendix A.1. Determination of a repulsive quasi-potential associated with Lamb shift for EDOs

Here we give only a schematic view of a work started on the occasion of a presentation at the 13th International Workshop on Anomalies in Hydrogen Loaded Metals (5–9 Oct. 2018, Grecchio, Italy). We build a repulsive potential as a function of the electron orbit radius from calculations on Self-energy (SE), which has a repulsive effect, while considering Vacuum Polarization (VP) calculations lead to a weakening of SE, since VP, which has an attractive effect, has to be subtracted from SE.

Appendix A.1.1. *The starting point of our method*

Our method consists of analyzing the progressions of SE and VP for atomic electrons for nuclei with increasing Z and, for comparisons and extrapolations, we consider the radius corresponding to the maximum probability density, noted *rmx*. Then, we consider the "Z increases" are equivalent to the "radius r decreases": Z increasing $\Leftrightarrow$ the coupling force increases $\Leftrightarrow$ the radius *rmx* decreases.

Nevertheless, as a deep electron is very far from an atomic electron, we use an *intermediate step* in terms of strength of the Coulomb electric field: the hydrogen-like uranium ion. This allows us to section the "distance" between an atomic case and a deep orbit, and above all, to take advantage of many calculations and experiments on the Lamb shift (LS) for heavy elements. Nevertheless, we have to be careful, because, for heavy elements, LS often includes terms that are not radiative corrections: for example, the nuclear size (NS), which has a significant effect. So, to calculate the LS for deep electrons, we discard any effect other than SE and VP.

Note: from now on, we consider the LS only for 1s electrons, for any chemical elements.

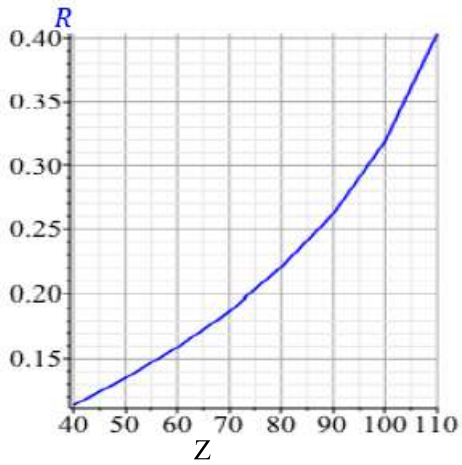

Figure 8. Smooth plot of ratio $R = |\text{VP}|/\text{SE}$, as function of Z, from data given in [45] and for $40 \leq Z \leq 110$.

In Fig. 7 we plot the normalized radial probability density for the 1s orbital of uranium, for $\rho < 2$ pm. For uranium, the radius corresponding to the maximum density probability, noted *rmx*(U) is equal to ∼427.3 F.

As indicated in Section 4.3 on radiative corrections, the energy shift due to SE can be expressed by the following formula: $\Delta E_{\text{LS}} = (\alpha/\pi)(Z\alpha)^4 \text{F}(Z\alpha)\, mc^2$. This formula has two factors depending on Z. The first, $(Z\alpha)^4$, quickly increases with the electric Coulomb field and can lead to a possible analytic formulation as function of the radius r.

From data tables, one can see the second factor, $F(Z\alpha)$, slowly decreases with Z. Moreover, again from a table of results, the ratio |VP|/SE increases with Z.

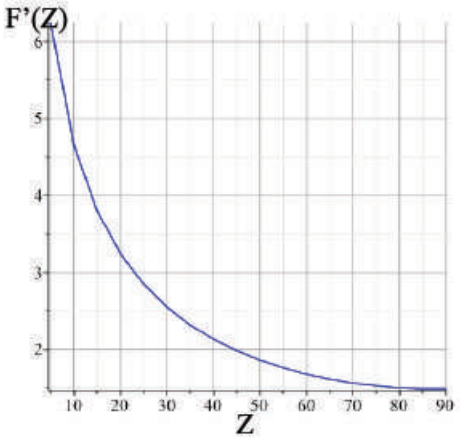

Figure 9. Smooth plot of factor $F'(Z)$, as function of Z, from data given in [42] and for $5 \leq Z \leq 90$.

Appendix A.1.2. *The form of the analytic expression of SE, and extrapolations from data tables*

Elements of comparison between SE values for the hydrogen atom and uranium lead us to take SE = C/r^3 as more "reasonable" than C/r^4. And, we can expect the reducing of SE to the power 3 can be "absorbed" thanks to the progression of |VP|/SE. We give in Fig. 8, a smooth plot of the ratio $R = |\text{VP}|/\text{SE}$, as function of Z, from [45]

With the data table, from $Z = 40$, we can recognize and extrapolate a slow geometric progression of the form $R_n = R_0 q^n$, where $q \sim 1.2$, $R_0 = R(Z = 40)$ and $n = (Z - 40)/10$. Thus it can compensate the reduction of SE indicated above, without having to subtract |VP| from SE. Next, we consider the factor $F(Z\alpha)$, expressed more simply as $F'(Z)$. In Fig. 9, we give a smooth plot of $F'(Z)$, built from [42], for $5 \leq Z \leq 90$.

From the data table, we can recognize and extrapolate a quasi-exponential decreasing progression of the factor $F'(Z)$, while considering the progression of Z multiplied by successive integer powers of *2*, from $Z = 5$: in fact, at each step, $F'(Z)$ is divided by a number k which is very slowly increasing. To sum up, while considering the ratio of *rmx*(U) $/r_{\text{edo}}$, where r_{edo} is an expected value of the LME for an EDO, fixed to ∼1.4 F, the factor $F'(92)$ ∼1.49 for uranium, and SE = 355 eV for uranium, we obtain an approximate value of F' for an EDO, noted F'_{edo} ∼0.021. From F'_{edo}, we deduce $V_{\text{LS}} \sim 6.2 \times 10^{-56}/r^3$ in SI units or $V_{\text{LS}} \sim 3.8 \times 10^{-37}/r^3$ in eV (with *r* in meters).

Acknowledgements

The authors wish to thank the reviewer for pointing out the problems associated with the spin magnetic moment of a relativistic electron. This work is supported in part by HiPi Consulting, Windsor, VA, USA and by the Science for Humanity Trust Inc., Tucker, GA, USA.

References

[1] M. Fleishmann and S. Pons, Electrochemically induced nuclear fusion of deuterium, *J. Electroanal. Chem.* **261**(1989) 301.
[2] A. Meulenberg and K.P. Sinha, Tunneling beneath the ^{4}He$*$ fragmentation energy, presented at 239th ACS National Meeting, San Francisco, CA March 2010, *J. Condensed Matter Nucl. Sci.* **4** (2011) 241–255.
[3] K.P. Sinha and A. Meulenberg, Lochon Catalyzed D–D fusion in deuterated palladium in the solid state, *National Academy of Sci. (India) Lett.* **30** (7,8) (2007) arXiv:0705.0595v1.
[4] K.P. Sinha and A. Meulenberg, A model for enhanced fusion reaction in a solid matrix of metal deuterides, *Proc. of the 14th Int. Conf. on Cold Fusion (ICCF-14)*, 10-15 Aug. 2008, Washington DC, p. 633.
[5] K.P. Sinha, Model of low energy nuclear reactions in a solid matrix with defects, PDF Special Section: Low Energy Nuclear Reactions, Section editors: M. Srinivasan and A. Meulenberg, *Current Sci.* **108** (4) (2015) 516, available at http://www.currentscience.ac.in/cs/php/feat.php?feature=Special%20Section:%20Low%20Energy%20Nuclear%20Reactions&featid=100
[6] A. Meulenberg and K.P. Sinha, Composite model for LENR in linear defects of a lattice, ICCF-18, *18th Int. Conf. on Condensed Matter Nucl. Sci.*, Columbia, Missouri, 25/07/2013, http://hdl.handle.net/10355/36818.
[7] E. Storms, How basic behavior of LENR can guide. A Search for an explanation, *J. Condensed Matter Nucl. Sci.* **20** (2016) 100, www.iscmns.org/CMNS/JCMNS-Vol20.pdf and the references therein.
[8] A. Takahashi, Physics of cold fusion by TSC theory, *J. Condensed Matter Nucl. Sci.* **12** (2013) and https://www.researchgate.net/publication/311614659_Physics_of_Cold_Fusion_by_TSC_Theory_full_paper.
[9] J.L. Paillet and A. Meulenberg, The basis for electron deep orbits of the hydrogen atom, *ICCF-19, 19th Int. Conf. on Cond. Matter Nuclear Science*, Padua, Italy, 15/05/2015, *J. Condensed Matter Nucl. Sci.* **19**(2016) 230–243.
[10] J.L. Paillet and A. Meulenberg, Special relativity: the source of electron deep orbits, *Foundations of Physics*, Vol. 47, Issue 2, Springer, Heidelberg, Feb. 2017, pp. 256–264.
[11] J.L. Paillet and A. Meulenberg, Arguments for the anomalous solutions of the Dirac equations, *J. Condensed Matter Nucl. Sci.* **18** (2016) 50–75, http://viXra.org/abs/1506.0177.
[12] A. Meulenberg and J.L. Paillet, Physical reasons for rejecting arguments against deep-Dirac levels, *J. Condensed Matter Nucl. Sci.* **24** (2017) 230–235.

[13] A. Meulenberg, Femto-atoms and transmutation, *17th Int. Conf. on Condensed Matter Nucl. Sci.*, Daejeon, South Korea, 12–17 August, 2012, *J. Condensed Matter Nucl. Sci.* **13** (2014) 346–357.

[14] A. Meulenberg and K.P. Sinha, Deep-orbit-electron radiation emission in decay from 4He*# to 4He, *17th Int. Conf. on Condensed Matter Nucl. Sci.*, Daejeon, South Korea, 12–17 August, 2012, *J. Condensed Matter Nucl. Sci*. **13** (2014) 357–368.

[15] A. Meulenberg and K.P. Sinha, New visions of physics through the microscope of cold fusion invited paper, *17th Int. Conf. on Condensed Matter Nucl. Sci.*, Daejeon, South Korea, 12–17 August, 2012, *J. Condensed Matter Nucl. Sci.* **13** (2014) 378–390.

[16] A. Meulenberg and K.P. Sinha, Deep-electron orbits in Cold Fusion, *17th Int. Conf. on Condensed Matter Nucl. Sci.*, Daejeon, South Korea, 12–17 August, 2012, *J. Condensed Matter Nucl. Sci.* **13** (2014) 368–377.

[17] A. Meulenberg, Extensions to physics: what cold fusion teaches, *Special Section: Low Energy Nuclear Reactions,* Section, M. Srinivasan and A. Meulenberg (Eds.), *Current Science,* Vol. 108, No. 4, 25 Feb. 2015. http://www.currentscience.ac.in/cs/php/feat.php?feature=Special%20Section:%20Low%20Energy%20Nuclear%20Reactions&featid=100

[18] A. Meulenberg, Femto-helium and PdD transmutation, *ICCF-18, 18th Int. Conf. on Condensed Matter Nucl. Sci.*, Columbia, Missouri, 25/07/2013, *J. Condensed Matter Nucl. Sci.* **15** (2015) 106–117.

[19] A. Meulenberg and J.L. Paillet, Basis for femto-molecules and -ions created from femto-atoms, *ICCF-19, 19th Int. Conf. on Condensed Matter Nucl. Sci.*, Padua, Italy, 15/05/2015, *J. Condensed Matter Nucl. Sci*. **19** (2016) 202–209.

[20] A. Meulenberg and J.L. Paillet, Implications of the electron deep orbits for cold fusion and physics, *J. Condensed Matter Nucl. Sci.* **24** (2017) 214–229.

[21] J.L. Paillet and A. Meulenberg, Electron deep orbits of the hydrogen atom, *Proc. 11*$^{\text{th}}$ *Int. Workshop on Hydrogen Loaded Metals*, Airbus Toulouse, France, 15–16 Oct. 2015, *J. Condensed Matter Nucl. Sci.* **23** (2017) 62–84.

[22] J.L. Paillet and A. Meulenberg, Advance on electron deep orbits of the hydrogen atom for LENR, *Proc. ICCF-20, 20th Int. Conf. on Condensed Matter Nucl. Sci.*, Sendai, Japan, October 2–7 2016, *J. Condensed Matter Nucl. Sci.* **24** (2017) 258–277.

[23] J.L. Paillet and A. Meulenberg, Deepening questions about electron deep orbits of the hydrogen atom, *Proc. 12*$^{\text{th}}$ *Int. Workshop on Hydrogen Loaded Metals*, Asti, Italy, June 5–9 2017, *J. Condensed Matter Nucl. Sci.* **26** (2018) 54–68.

[24] A. Messiah, *Quantum Mechanics*, Vol. 1, North-Holland, Amsterdam, 1967.

[25] Cl. Cohen-Tannoudji, B. Diu and Fr. Laloë, *Quantum Mechanics*, Vol. 1, C_I, Wiley-VCH, New York, London, Sydney, Toronto, 1977.

[26] S.V. Adamenko and V.I. Vysotskii, Mechanism of synthesis of superheavy nuclei via the process of controlled electron-nuclear collapse, *Foundations Phys. Lett.* **17** (3) (2004) 203–233.

[27] S.V. Adamenko and V.I. Vysotskii, Evolution of annular self-controlled electron–nucleus collapse in condensed targets, Foundations Phys. **34** (11) (2004) 1801–1831.

[28] [28] J.L. Paillet and A. Meulenberg, Relativity and Electron deep orbits of the hydrogen atom, *Proc. of the 1st French Symp. RNBE-2016 on Condensed Matter Nucl. Sci.*, Avignon, 18–20 March 16, *J. Condensed Matter Nucl. Sci.* **21** (2016) 40–58.

[29] L.I. Schiff, *Quantum Mechanics*, 3rd Edn., McGraw-Hill, New York, 1968.

[30] Cl. Cohen-Tannoudji, B. Diu and Fr. Laloë, *Quantum Mechanics*, Vol. 2, Ch. XII B, Wiley-VCH, Hoboken, New-Jersey, 1977.

[31] H. Murayama, *Quantum Mechanics*, 221A Lecture Notes, Fall, 2006, Berkeley, http://hitoshi.berkeley.edu/221a/hyperfine.pdf, last access: Sep. 2018.

[32] R. Klauber, *Student Friendly Quantum Field Theory*, 2nd. Edn., Sandtrove Press, Fairfield, Iowa, 2013.

[33] W.H.E. Schwarz, An Introduction to Relativistic Quantum Chemistry, *Relativistic Methods for Chemists*, Chapter 1, *Challenges and Advances in Comp. Chem. and Phys. Series*, J. Leszczynski (Ed.), Vol. 10, Ed. By M. Barysz, Yasuyuki Ishikawa, Springer, Berlin, 2010.

[34] Cl. Cohen-Tannoudji, B. Diu and Fr. Laloë, *Quantum Mechanics*, Vol. 2, Ch. VII, D_{VII}, Wiley-VCH, Hoboken, New-Jersey, 1977.

[35] F. Mandl and G. Shaw, *Quantum Field Theory*, 2nd. Edn., Wiley, Chichester, UK, 2010.

[36] J.M. Jauch and F. Rohrlich, *The Theory of Photons and Electrons*, Addison-Wesley, Reading, USA, 2nd., Printing, June 1959.

[37] W.H. Furry, On bound states and scattering in positron theory, *Phys. Rev.* **81** (1951) 115.

[38] W. Lamb and R. Retherford, Fine structure of the hydrogen atom by a microwave method, *Phys. Rev.* **72**(3) (1947) 241–243.
[39] H.A. Bethe, The electromagnetic shift of energy levels, *Phys. Rev.* **72** (1947) 337.
[40] F.J. Dyson, *Advanced Quantum Mechanics*, 2nd. Edn., arXiv:quant-ph/0608140v1 18 Aug. 2006.
[41] A. Meulenberg, W.R. Hudgins and R.F. Penland, The photon to electron/positron-pair transition, *Proc. SPIE*. 9570, The Nature of Light: What are Photons? VI, 95700S, September 10, 2015, doi: 10.1117/12.2187489.
[42] P.J. Mohr, Self-energy correction to one-electron energy levels in a strong Coulomb field, *Phys. Rev.* **46** (7)(1992)4421–4424.
[43] P.J. Mohr, Quantum electrodynamics calculations in few-electron systems, *Phys. Scripta* **46**(1993) 44–51.
[44] A.M. Frolov and D. Wardlaw, Analytic formula for the Uehling potential, arXiv:1110.3433v4 [nucl-th] (2012).
[45] W.R. Johnson and G. Soff, The Lamb shift in hydrogen-like atoms, $1 \leq Z \leq 110$, *Atomic Data and Nuclear Data Tables*, Vol. 33, Academic Press, New York, 1985, pp. 405–446.
[46] Virial Theorem. https://en.wikipedia.org/wiki/Virial_theorem, 3 Sept. 2018.
[47] Cl. Cohen-Tannoudji, B. Diu and Fr. Laloë, *Quantum Mechanics*, Vol. 2, Ch. X, Fx, Wiley-VCH, New York, 1977.
[48] Strassler Matt., Checking What's Inside a Proton, in Blog Of Particular Significance. https://profmattstrassler.com/articles-and-posts/largehadroncolliderfaq/whats-a-proton-anyway/checking-whats-inside-a-proton/, last access: Sept. 2018.
[49] [49]J. Martin Victoria, Probing the Proton: Electron–Proton Scattering, Lect. 8, Collider Physics, University of Edinburgh, results from HERA collider DESY in Hamburg, 2012. https://www2.ph.ed.ac.uk/~vjm/Lectures/SHParticlePhysics2012_files/PPNotes3.pdf, last access: Sept 2018.
[50] J. Beringer (*Particle Data Group*) et al. 2012, *PDGLive Particle Summary 'Quarks'*, PR **D86**, 010001 (2012), http://pdg.lbl.gov, last access: Sept. 2018.
[51] D. Diakonov, Foundations of the constituent quark model, *Prog. Part. Nucl. Phys.* **36** (1996) 1–18, arXiv:nucl-th/9603023v1, 17 Mar. 1996.
[52] W. Zawadski, Spin magnetic moment of a free relativistic electron, *Phys. Rev.* D **3** (8) (1971) 1728.
[53] S. Sasabe, Spin-magnetic moment of dirac electton and role of Zitterbewegung, *J. Modern Phys.* (2014) 534–542.